

Magnetotransport and electronic noise in superparamagnetic magnetic tunnel junctions

Cite as: Appl. Phys. Lett. **115**, 022402 (2019); <https://doi.org/10.1063/1.5110715>

Submitted: 20 May 2019 • Accepted: 21 June 2019 • Published Online: 08 July 2019

Yiou Zhang,  Guanyang He, Xixiang Zhang, et al.



View Online



Export Citation



CrossMark

ARTICLES YOU MAY BE INTERESTED IN

[PicoTesla magnetic tunneling junction sensors integrated with double staged magnetic flux concentrators](#)

Applied Physics Letters **113**, 242401 (2018); <https://doi.org/10.1063/1.5052355>

[Noise characterization of ultrasensitive anomalous Hall effect sensors based on \$\text{Co}_{40}\text{Fe}_{40}\text{B}_{20}\$ thin films with compensated in-plane and perpendicular magnetic anisotropies](#)

Applied Physics Letters **116**, 212404 (2020); <https://doi.org/10.1063/5.0008949>

[Superparamagnetic perpendicular magnetic tunnel junctions for true random number generators](#)

AIP Advances **8**, 055903 (2018); <https://doi.org/10.1063/1.5006422>



Time to get excited.
Lock-in Amplifiers – from DC to 8.5 GHz

[Find out more](#)

 Zurich Instruments

Magnetotransport and electronic noise in superparamagnetic magnetic tunnel junctions

Cite as: Appl. Phys. Lett. **115**, 022402 (2019); doi: [10.1063/1.5110715](https://doi.org/10.1063/1.5110715)

Submitted: 20 May 2019 · Accepted: 21 June 2019 ·

Published Online: 8 July 2019



View Online



Export Citation



CrossMark

Yiyou Zhang,¹ Guanyang He,¹  Xixiang Zhang,² and Gang Xiao^{1,a)}

AFFILIATIONS

¹Department of Physics, Brown University, Providence, Rhode Island 02912, USA

²Division of Physical Science and Engineering, King Abdullah University of Science and Technology, Thuwal 239955, Kingdom of Saudi Arabia

^{a)}Email: Gang_Xiao@brown.edu

ABSTRACT

We have investigated the magnetotransport and noise properties of magnetic tunnel junctions incorporating a superparamagnetic free layer, in a wide temperature range from 150 K to 400 K. Both $1/f$ noise and sensitivity reach the maximum near the blocking temperature of the superparamagnetic transition. The smooth change of noise around the blocking temperature is attributed to size distribution of nanoclusters comprising the free layer. The best detectability ($40 \text{ nT}/\sqrt{\text{Hz}}$ at 1 Hz) is achieved at 350 K. In ferromagnetic and superparamagnetic states, $1/f$ noise follows different scaling relations with respect to sensitivity. The change of scaling law is explained by thermodynamics of the nanoclusters.

Published under license by AIP Publishing. <https://doi.org/10.1063/1.5110715>

For sensitive magnetic field sensors with a small size and mass-production potential, a magnetic tunnel junction (MTJ) sensor is a promising candidate, which has been shown to have picotesla detectability at room temperature.^{1–6} To reach better sensing detectability, it is essential to study the intrinsic noise of MTJs. The intrinsic noise may also give more information on defects and magnetic dynamics of MTJs than simple transport measurements.^{7–9} Besides typical application in spintronics and magnetic recording, MTJ sensors can also be used for biomedical and automotive applications, where low-frequency signals are of interest. At low frequency, the $1/f$ noise of MTJ dominates; yet, its mechanism is less understood. Two physical origins of $1/f$ noise have been proposed: an electron trap-and-release process due to defects in the tunnel barrier layer or at interfaces (electronic $1/f$ noise) and thermally excited hopping of magnetic domain walls between metastable states (magnetic $1/f$ noise).^{9,10} It has been found that the latter is dominant in the sensing region of MTJs^{9–11} and therefore sets the sensing limit of MTJ-based sensors.

One approach to reduce this magnetic $1/f$ noise, which originates from a ferromagnetic electrode, is to switch to a superparamagnetic electrode. Through the reduction of the layer thickness, the free layer of MTJ breaks into magnetic clusters after thermal annealing.¹² Formation of such nanoclusters is attributed to the three-dimensional growth mode of Fe on MgO in the initial stage,¹³ as well as the presence of barrier steps on the MgO surface.¹⁴ As thermal fluctuation is

enough to overcome the anisotropy energy, magnetic moments in these magnetic clusters undergo coherent rotation under an external magnetic field. Superparamagnetic MTJs are appealing due to the linear and hysteresis-free behavior.^{14–16} Also, negligible magnetic $1/f$ noise has been observed in MTJs with thin superparamagnetic free layers.^{17–19} This is attributed to the elimination of domain walls in the superparamagnetic free layer. Nevertheless, these studies on superparamagnetic MTJs usually suffer from a lack of data, as the measurements are merely done with only a few samples of discrete free layer thicknesses. Since superparamagnetism exhibits a strong temperature dependence,^{14,19} it is more effective to study ferromagnetic-to-superparamagnetic transition by varying the measurement temperature continuously. While the temperature dependence of transport properties of superparamagnetic MTJ has been reported,¹⁴ the temperature effect of its intrinsic noise has not been revealed. In this work, we performed a more systematic analysis on the magnetotransport properties and noise behavior across the transition from ferromagnetic to superparamagnetic free layers through continuous variation of the measurement temperature. We found that sensitivity and $1/f$ noise of superparamagnetic MTJs show different dependences on the temperature and bias magnetic field. This gives rise to an oscillatory behavior of the field detectability, which goes as low as $40 \text{ nT}/\sqrt{\text{Hz}}$ at 1 Hz at 350 K. Moreover, different scaling relations between $1/f$ noise and sensitivity have been observed in ferromagnetic and superparamagnetic

states. The transition of the scaling relation is explained by the thermodynamics of magnetic nanoparticles.

We fabricated our MTJ stacks according to the layer sequence of Si substrate/SiO₂/Ta(50)/Ru(300)/Ta(50)/Co₅₀Fe₃₀(30)/IrMn(180)/Co₅₀Fe₃₀(30)/Ru(8.5)/Co₄₀Fe₄₀B₂₀(*t_{pin}*)/MgO(29)/Co₄₀Fe₄₀B₂₀(*t_{free}*)/Ta(100)/Ru(100), where the numbers in parentheses represent the nominal thickness of each layer in angstroms. The stacks were then patterned into MTJ sensors by using standard photolithography and physical ion milling. Each MTJ sensor consists of 4 MTJs in series, each of which has an oval shape of 15 × 120 μm². Thermal annealing at 300 °C under an external magnetic field of 0.42 T was performed in the end of the fabrication. More details of MTJ fabrication can be found in our previous work.^{6,20} The magnetotransport properties at room temperature are measured on a probe station equipped with a pair of calibrated electromagnets. For the temperature dependence study, a Quantum Design[®] Physical Property Measurement System (PPMS) is used to set temperature from 150 K to 400 K, as well as the external magnetic field from −7 T to 7 T. A block diagram of the noise measurement system is shown in Fig. 1(a). A 3 V battery in series with a low-temperature-coefficient resistor is used to apply bias voltage (0.5–1 V) on MTJ. The AC output of MTJ is amplified by two preamplifiers inside the PPMS sample chamber and then further amplified at room temperature. A cross-correlation method is used to cancel noise from the amplifiers.²¹ One additional DC amplifier is used to read out the DC bias voltage on MTJ. Resistance of the MTJ at a given temperature and magnetic field is also determined from the DC bias voltage and resistance of the serial resistor. The noise measurement system is calibrated by measuring thermal noise of various resistors at different temperatures, and a negligible background noise of 3 nV/√Hz is determined. One typical noise spectrum of an MTJ device is shown in Fig. 1(b). In the whole frequency range (1 Hz–10 kHz), MTJ noise is much larger than the background noise, which justifies our noise measurement results.

Figure 2(a) shows the tunneling magnetoresistance ratio (TMR) of MTJ samples measured at room temperature, with different free layer thicknesses *t_{free}* from 10 Å to 15 Å and *t_{pin}* = 30 Å. With decreasing *t_{free}*, the TMR value drops rapidly. Different offset magnetic fields are also observed, which can be attributed to the changes in the inter-layer coupling fields.^{14,16} The coercivity disappears after *t_{free}* drops below a critical thickness around 12.5 Å, indicating a magnetic transition of the free layer from ferromagnetism to superparamagnetism. For the rest of this paper, we choose *t_{free}* = 12.5 Å and *t_{pin}* = 25 Å to

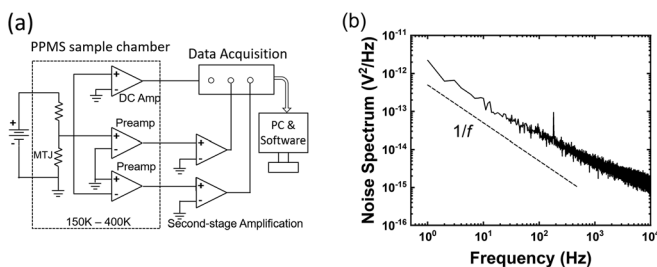


FIG. 1. (a) Block diagram of the noise measurement setup. (b) One typical noise spectrum of MTJ (measured at zero magnetic field at 300 K) at a bias voltage of 0.7 V.

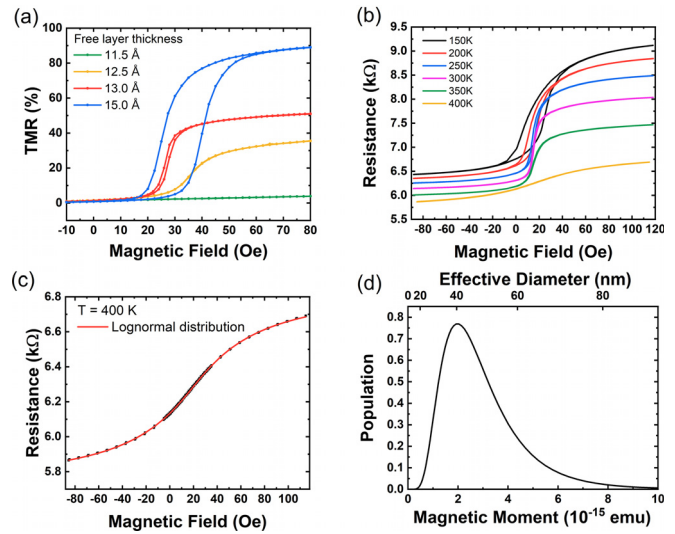


FIG. 2. (a) Transfer curve of MTJs with different free layer thicknesses, measured at room temperature. (b) Transfer curves of MTJ with a free layer thickness of 12.5 Å and temperatures from 150 K to 400 K. (c) Fitting of the transfer curve at 400 K with the Langevin function. The red line assumes that the nanocluster size follows a lognormal distribution. (d) Magnetic cluster size distribution obtained from the red line in (c). The effective diameter of the nanoclusters is computed under the assumption that each nanoparticle is of cylindrical shape with a height of 12.5 Å.

reduce the offset magnetic field. Figure 2(b) shows the transfer curve from 150 K to 400 K. At 300 K and 350 K, hysteresis has already dropped to minor values but can still be observed. To confirm its superparamagnetic state, we fit the transfer curve at 400 K with the equation deduced from magnetotunneling theory and the Langevin equation of superparamagnetism,^{12,16}

$$R(H) = C_1 L\left(\frac{m(H - H_0)}{k_B T}\right) + C_2, \quad (1)$$

where T is the temperature, k_B is Boltzmann's constant, m is the magnetic moment of one magnetic cluster in the free layer, H_0 is the offset magnetic field, and C_1 and C_2 are two fitting constants. We assume that the magnetic moment of the cluster is proportional to its size and the nanocluster size follows a lognormal distribution.¹³ The resulting red fitting line, shown in Fig. 2(c), gives an excellent match with all the data points. This implies that size variation of the nanoclusters is an important factor. The obtained magnetic moment distribution is shown in Fig. 2(d), with an average magnetic moment of 2.4×10^{-15} emu. From the saturation magnetization of CoFeB (1240 emu/cm³), we can estimate the average volume of nanoclusters to be 2.0×10^{-18} cm³, or an effective diameter of 45 nm, much smaller than the free-layer volume (5.9×10^{-12} cm³) assuming a continuous free layer. Therefore, the free layer is a large number of superparamagnetic nanoclusters.

Besides magnetotransport properties, voltage noise of MTJ was also measured as the magnetic field was swept from 118 Oe to −88 Oe. The low-frequency noise of MTJ, shown in Fig. 3(a), has a strong dependence on both the bias field and temperature. In the saturation region, $1/f$ noise of MTJ increases monotonically with temperature, which can be understood from the enhanced thermal fluctuation

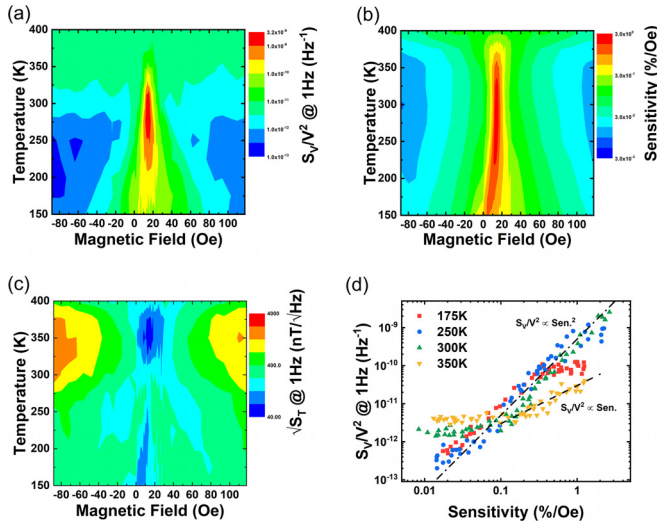


FIG. 3. (a) The map of voltage normalized noise at 1 Hz, (b) sensitivity map, and (c) the map of field detectability at 1 Hz. (d) Plot of normalized noise vs sensitivity on a log-log scale.

of the defects. In the sensing region, the $1/f$ noise first increases and then decreases with temperature. If we compare the $1/f$ noise in the sensing region, we can see that the $1/f$ noise is lower at high temperatures (superparamagnetic state) than that at low temperatures (ferromagnetic state). This implies that the MTJ in the superparamagnetic state has lower magnetic $1/f$ noise. However, $1/f$ noise appears to change rather smoothly near the blocking temperature, which is not the boundary of a phase transition, but a manifestation of slowing magnetic relaxation rate vs instrument’s measuring time. Such a broadening effect can be understood from the size distribution of nanoclusters.²² As temperature rises, more nanoclusters become superparamagnetic and their magnetic $1/f$ noise is reduced. On the other hand, the remaining ferromagnetic nanoclusters give larger magnetic $1/f$ noise due to the enhanced thermal-magnetic fluctuation. The competition between these two processes leads to a smooth change of $1/f$ noise with respect to temperature. It should be pointed out that the broadening effect may also originate from dipole interaction between nanoclusters.^{23,24} When temperature is around 400 K, the electronic $1/f$ noise becomes larger than the magnetic $1/f$ noise under any bias field, giving rise to bias field-independent $1/f$ noise. Similar behavior has been observed in previous work on superparamagnetic MTJs.^{17–19}

Apart from the intrinsic noise, we can also calculate the sensitivity of MTJ through

$$s = \frac{1}{R} \frac{dR}{dH}, \quad (2)$$

which gives the sensitivity map shown in Fig. 3(b). It should be noted that the sensitivity based on this calculation may be overestimated due to the finite coercivity, as found in previous work.^{5,6,19,25} At $T < 350$ K, sensitivity shows a strong dependence on the bias field, yet only changes slightly with respect to temperature. At $T > 350$ K, sensitivity of MTJ drops rapidly, as magnetic susceptibility of superparamagnetic nanoclusters declines at higher temperatures. This is in contrast to $1/f$ noise of MTJ, which shows a strong temperature dependence at all

measurement temperatures. Combining the voltage noise (S_V) and the sensitivity (s), we can determine the field detectability (or field noise) as

$$S_T \left(\frac{T^2}{\text{Hz}} \right) = \frac{S_V}{V^2 s^2}, \quad (3)$$

which is plotted in Fig. 3(c). Compared to voltage noise and sensitivity, the field detectability shows a more complex dependence on temperature. The best field detectability (40 nT/ $\sqrt{\text{Hz}}$ at 1 Hz) is obtained at $T = 350$ K, rather than $T \sim 300$ K, where sensitivity is the largest, or $T \sim 400$ K, where noise is smaller.

To better understand this, the voltage normalized noise is plotted against sensitivity at various temperatures, shown in Fig. 3(d). Interestingly, the voltage normalized noise scales linearly with sensitivity at high temperature, yet quadratically with sensitivity at low temperature. From the theoretical model based on fluctuation-dissipation theorem, a linear relation between $1/f$ noise and sensitivity is expected and has been experimentally observed.^{9,26} However, such a prediction relies on thermodynamic equilibrium, which generally does not hold for ferromagnetic systems. Indeed a quadratic relation has also been observed in MTJs with a ferromagnetic free layer in previous work.^{10,25,27,28} There have been no reports on the scaling relation in superparamagnetic MTJs. Since the linear scaling relation is observed only in the superparamagnetic state, we suspect that the nanoclusters reach thermal equilibrium only when they become superparamagnetic. The reason behind the quadratic scaling law for ferromagnetic systems remains an open question. The scaling law relation is important for MTJ performance. As can be seen from Eq. (3), if voltage noise scales quadratically with sensitivity, field detectability becomes constant and does not improve as sensitivity increases. On the other hand, if voltage noise scales linearly with sensitivity, field detectability can be improved through increasing sensitivity. Therefore, a linear relation between voltage noise and sensitivity is desirable for optimal performance of MTJ. In order to obtain such a linear relationship, the majority of nanoclusters should become superparamagnetic. This means that the temperature should be high enough so that nanoclusters of relatively large size are superparamagnetic. However, such high temperatures reduce the magnetic susceptibility of small nanoclusters, thus decreasing the sensitivity of MTJ. This can be observed from Figs. 3(b) and 3(d). When sensitivity is maximum (3%/Oe at $T = 300$ K), voltage noise scales quadratically with sensitivity, which results in poor field detectability. When voltage noise starts to scale linearly with sensitivity ($T = 350$ K), sensitivity is reduced to 1%/Oe, which limits further improvement on field detectability. If all the nanoclusters can be made of the same size, the linear scaling relation between noise and sensitivity can be realized before sensitivity is largely reduced. Under such a condition, MTJ could have high sensitivity as well as low $1/f$ noise. Therefore, a more uniform size distribution of the nanoclusters would be highly beneficial for the performance of superparamagnetic MTJs.

In summary, we have fabricated MTJs with a superparamagnetic free layer and measured its magnetotransport properties and noise spectrum over a broad range of magnetic fields and temperatures. From the transfer curve of MTJ at 400 K, we have obtained the size distribution of magnetic nanoclusters, which compose the free layer of MTJ. The size variation of nanoclusters is shown to be important in order to understand the change in both noise and sensitivity with respect to the bias magnetic field and temperature. The best

detectability ($40 \text{ nT}/\sqrt{\text{Hz}}$ at 1 Hz) is achieved at 350 K where the MTJ becomes superparamagnetic. Moreover, a transition from the quadratic scaling relation to the linear scaling relation between voltage normalized noise and sensitivity has been explored. These findings shall provide guidelines to understanding fundamental physics of superparamagnetic nanoclusters as well as to improving MTJ sensing performance.

This work was supported by the King Abdullah University of Science and Technology (KAUST) through the Sensor Initiative.

REFERENCES

- ¹R. C. Chaves, P. P. Freitas, B. Ocker, and W. Maass, *Appl. Phys. Lett.* **91**, 102504 (2007).
- ²S. H. Liou, X. L. Yin, S. E. Russek, R. Heindl, F. C. S. Da Silva, J. Moreland, D. P. Pappas, L. Yuan, and J. Shen, *IEEE Trans. Magn.* **47**, 3740 (2011).
- ³J. P. Valadeiro, J. Amaral, D. C. Leitao, R. Ferreira, S. F. Cardoso, and P. J. P. Freitas, *IEEE Trans. Magn.* **51**, 1 (2015).
- ⁴S. Cardoso, D. C. Leitao, L. Gameiro, F. Cardoso, R. Ferreira, E. Paz, and P. P. Freitas, *Microsyst. Technol.* **20**, 793 (2014).
- ⁵X. Yin, Y.-F. Liu, D. Ewing, C. K. Ruder, P. J. De Rego, A. Edelstein, and S.-H. Liou, *Spintronics VIII* (International Society for Optics and Photonics, 2015), p. 95512N.
- ⁶G. Y. He, Y. Zhang, L. J. Qian, G. Xiao, Q. Zhang, J. C. Santamarina, T. W. Patzek, and X. X. Zhang, *Appl. Phys. Lett.* **113**, 242401 (2018).
- ⁷S. Garzon, Y. Chen, and R. A. Webb, *Physica E* **40**, 133 (2007).
- ⁸Z. Q. Lei, G. J. Li, W. F. Egelhoff, P. T. Lai, and P. W. T. Pong, *IEEE Trans. Magn.* **47**, 602 (2011).
- ⁹L. Jiang, E. R. Nowak, P. E. Scott, J. Johnson, J. M. Slaughter, J. J. Sun, and R. W. Dave, *Phys. Rev. B* **69**, 054407 (2004).
- ¹⁰C. Ren, X. Y. Liu, B. D. Schrag, and G. Xiao, *Phys. Rev. B* **69**, 104405 (2004).
- ¹¹G. Q. Yu, J. F. Feng, H. Kurt, H. F. Liu, X. F. Han, and J. M. D. Coey, *J. Appl. Phys.* **111**, 113906 (2012).
- ¹²J. W. Cao, Y. Liu, Y. Ren, F. L. Wei, and P. P. Freitas, *Appl. Surf. Sci.* **314**, 443 (2014).
- ¹³F. Ernult, K. Yamane, S. Mitani, K. Yakushiji, K. Takanashi, Y. K. Takahashi, and K. Hono, *Appl. Phys. Lett.* **84**, 3106 (2004).
- ¹⁴Y. Jang, C. Nam, J. Kim, B. Cho, Y. Cho, and T. Kim, *Appl. Phys. Lett.* **89**, 163119 (2006).
- ¹⁵P. Wisniewski, J. M. Almeida, S. Cardoso, N. P. Barradas, and P. P. Freitas, *J. Appl. Phys.* **103**, 07A910 (2008).
- ¹⁶W. F. Shen, B. D. Schrag, A. Girdhar, M. J. Carter, H. Sang, and G. Xiao, *Phys. Rev. B* **79**, 014418 (2009).
- ¹⁷J. M. Almeida and P. P. Freitas, *J. Appl. Phys.* **105**, 07E722 (2009).
- ¹⁸P. Wisniewski, J. M. Almeida, and P. P. Freitas, *IEEE Trans. Magn.* **44**, 2551 (2008).
- ¹⁹K. Ishikawa, M. Oogane, K. Fujiwara, J. Jono, M. Tsuchida, and Y. Ando, *Jpn. J. Appl. Phys., Part 1* **55**, 123001 (2016).
- ²⁰G. Xiao, in *Handbook of Spin Transport and Magnetism*, edited by E. Y. Tsymbal and I. Zutic (CRC Press, Taylor & Francis, Boca Raton, FL, USA, 2012).
- ²¹M. Sampietro, L. Fasoli, and G. Ferrari, *Rev. Sci. Instrum.* **70**, 2520 (1999).
- ²²Y. Park, S. Adenwalla, G. P. Felcher, and S. D. Bader, *Phys. Rev. B* **52**, 12779 (1995).
- ²³W. Luo, S. R. Nagel, T. Rosenbaum, and R. Rosensweig, *Phys. Rev. Lett.* **67**, 2721 (1991).
- ²⁴B. Mertens, K. Levin, and G. Grest, *Phys. Rev. B* **49**, 15374 (1994).
- ²⁵D. Mazumdar, X. Y. Liu, B. D. Schrag, M. Carter, W. F. Shen, and G. Xiao, *Appl. Phys. Lett.* **91**, 033507 (2007).
- ²⁶S. Ingvarsson, G. Xiao, S. S. Parkin, W. J. Gallagher, G. Grinstein, and R. H. Koch, *Phys. Rev. Lett.* **85**, 3289 (2000).
- ²⁷W. Z. Zhang, Q. Hao, and G. Xiao, *Phys. Rev. B* **84**, 094446 (2011).
- ²⁸D. Mazumdar, W. F. Shen, X. Y. Liu, B. D. Schrag, M. Carter, and G. Xiao, *J. Appl. Phys.* **103**, 113911 (2008).